Journal of Engineering and Applied Sciences 13 (17): 7408-7413, 2018
ISSN: 1816-949X

Linear and non Linear Analysis of the Impact of Emissivity and Distance on Hotspot Temperature in Condition Monitoring of Electrical Equipments by Thermal Imaging

[1]M.S. Sangeetha and [2]N.M. Nandhitha
[1]Sathyabama Institute of Science and Technology, Chennai, Tamil Nadu, India
[2]Faculty of Electrical and Electronics,
Sathyabama Institute of Science and Technology, Chennai, Tamil Nadu, India

Abstract: Condition monitoring of electrical equipments by infrared thermography is strongly dependent on the hotspot temperature. However, accuracy of hotspot detection is dependent not only on the image processing techniques for segmentation but is also dependent on the camera parameters (set during thermograph acquisition). Uncertainty in image processing techniques is reduced through multilevel contrast enhancement and improved active contour modeling. In order to remove uncertainty due to IR camera settings, mathematical relationships between the camera parameters and the error in temperature should be determined. In this study, three different techniques namely linear regression, back propagation network, curve fitting are used for deriving two dimensional equations. Though BPN and curve fitting provide non-linear relationship, curve fitting is favored as it results in accurate results and lesser computational complexity.

Key words: Emissivity, distance, error in temperature, back propagation network, curve fitting, hotspot temperature

INTRODUCTION

Infrared thermography is a non invasive, non contact, non hazardous technique, Non Destructive Testing (NDT) technique used for the quality assessment in industries (Maldague, 2002). It used an IR camera that captures heat and maps it into a 2D pattern called thermographs. In recent years, it is extensively used in condition monitoring of electrical equipment's. It is because, defects in electrical equipment's can be identified by studying the heat pattern. In order to perform condition monitoring, hot spot temperature of the equipment is measured and is plotted against time. This process is repeated for a period of time. If there is an abrupt variation in temperature (either increase or decrease) it indicates anomaly and it necessitates an inspection either immediately or after a period of time. Bedir *et al.* (2013) have proposed Graphical User Interface (GUI) with thermal imaging for detecting and solving the abnormal conditions in electrical circuit breakers. Suomela (2012) proposed condition motoring technique for paper rolling machines using adaptive triggering. Here, delayed pulse were used as external triggering signal to the camera for imaging the exact area of object surface. Schulz *et al.* (2014) proposed a methodology for monitoring rolling element bearings in wind turbines. Thermal images of rolling bearing at different running conditions were taken using IR thermal cameras and stored in a database. The inner raceway faults can be detected by high temperature variations. Hence, the exact location of faults was identified using IR images in wind turbines. Ullah *et al.* (2017) used machine learning approach for predictive maintenance of electrical systems in power station. Multilayered perceptron was used to classify the thermal conditions of electrical equipments into defect and non defect classes. The 84% accuracy was shown with the proposed technique.

However, thermal images taken form thermal camera suffer from operational and environmental conditions. Significant operational conditions which affect the hotspot temperature are emissivity and distance. In order to study the impact of the above parameters it is necessary to acquire images at varying distance and emissivity. Image processing techniques are then used to extract the hotspot and then temperature is determined using a conventional equation. Error between the actual temperature and calculated temperature is obtained. In this study, three different approaches are proposed to relate temperature with emissivity and distance.

MATERIALS AND METHODS

Temperature of the hotspot in thermographs is affected by uncertainty caused by the camera parameters (emissivity and distance) and uncertainty caused in hotspot extraction. Thermographs of USB

Corresponding Author: N.M. Nandhitha, Sathyabama Institute of Science and Technology, Chennai, Tamil Nadu, India

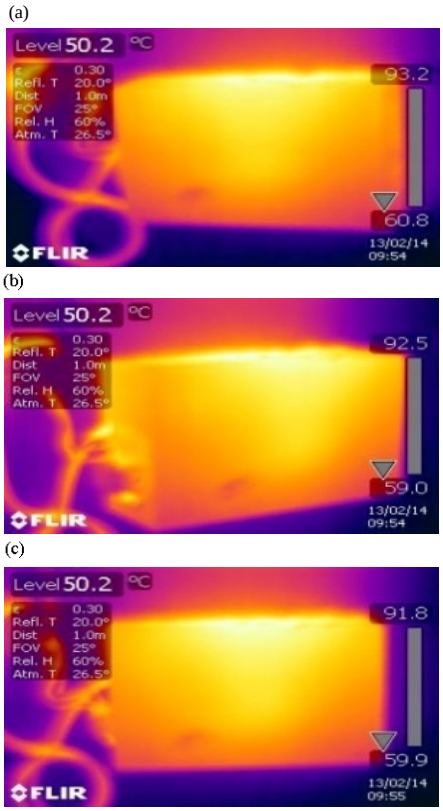

Fig. 1: IR thermograms of stabilizer at distance 1 m; a) Emissivity 0.6; b) Emissivity 0.7 and c) Emissivity 0.8

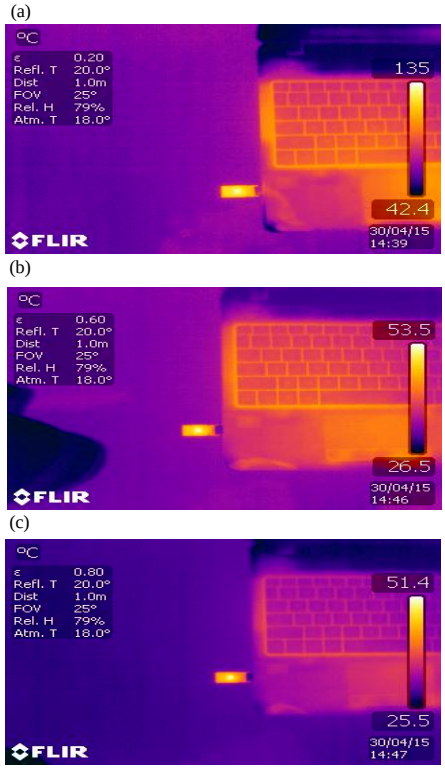

Fig. 2: IR thermograms of pen drive at distance 1 m a) Emissivity 0.2; b) Emissivity 0.6 and c) Emissivity 0

and stabilizer are acquired at different emissivity and distance. A set of 77 images at different emissivity and distance are acquired using FLIR T335. Acquired sample images are shown in Fig. 1 and 2.

Hotspot extraction: These pseudocolour thermographs are converted into gray scale images. Multilevel contrast enhancement is used to increase the contrast of gray scale images (Sangeetha and Nandhitha, 2016). Improved active contour modeling is used to segment the hotspot (Sangeetha and Nandhitha, 2017). Both multilevel contrast enhancement and improved active contour modelling has removed uncertainty in hotspot extraction. After extracting the hotspot, temperature is obtained using Eq. 1 (Bilodeau *et al*., 2011). Error in temperature is then determined by finding the difference between the hotspot temperature and the actual temperature. From the Fig. 3 and 4, it is found that the hotspot region is extracted to its true size:

$$T_{Real} = T_{Min} + (Average/255) \times (T_{Max} - T_{Min}) \quad (1)$$

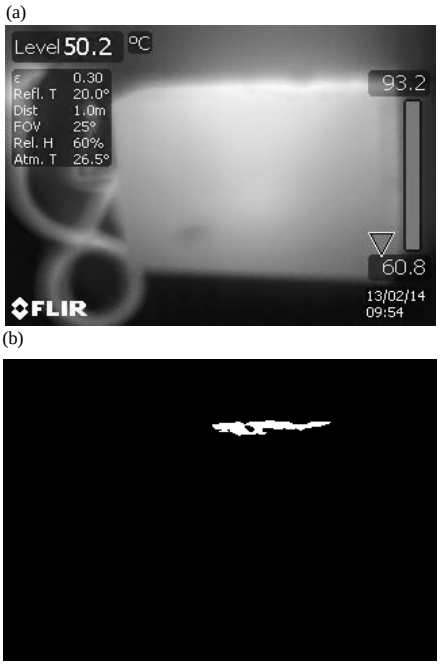

Fig. 3: Image of stabilizer at distance 1 m with emissivity 0.6; a) Grayscale image and b) Output image

Table 1: Relationship between emissivity, distance and hotspot temperature

Stabilizer			USB		
Emissivity	Distance (m)	Error in temperature (°C)	Emissivity	Distance (m)	Error in temperature (°C)
0.1	1	30.604	0.1	1.0	84.5212
0.2	1	34.920	0.1	0.9	80.6878
0.3	1	34.182	0.1	0.8	85.5805
0.4	1	34.665	0.1	0.7	86.4382
0.5	1	41.191	0.2	0.7	64.7030
0.6	1	9.396	0.2	0.8	64.9468
0.7	1	9.013	0.2	0.9	66.8899
0.8	1	8.785	0.2	1.0	68.1025
0.9	1	12.147	0.4	1.0	28.2383
1.0	1	6.678	0.4	0.9	12.4919
0.1	2	-4.838	0.4	0.8	1.5167
0.2	2	-5.750	0.6	1.0	-2.3349
0.3	2	-5.535	0.8	1.0	-4.7517
0.4	2	-2.946	0.8	0.9	-0.8404
0.5	2	-7.889	0.8	0.8	0.0068
0.6	2	-14.590	0.8	0.7	1.6892
0.7	2	-14.590	1.0	0.7	-4.0638
0.9	2	-11.930	1.0	0.8	-4.5715
1.0	2	-15.150	1.0	0.9	-4.3395
0.1	3	-22.450	1.0	1.0	-4.4499
0.2	3	-20.890			
0.3	3	-18.660			
0.4	3	-19.930			
0.5	3	-20.720			
0.6	3	-22.860			
0.7	3	-23.230			
0.8	3	-21.040			
0.9	3	-24.200			
1.0	3	-25.360			

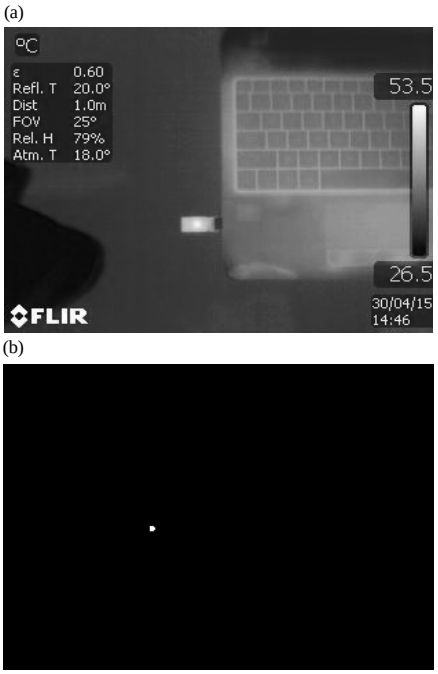

Fig. 4: Image of USB at distance 1 m with emissivity 0.6; a) Grayscale image and b) Output image

Mathematical relationship between emissivity, distance and error in temperature: Relationship between emissivity, distance and hotspot temperature are shown in Table 1. Initially one dimensional equations relating error in temperature with emissivity and with distance are determined (Sangeetha *et al*., 2014). In order to determine the utilization chart it is necessary to obtain two dimensional mathematical relationships between these camera parameters and error in temperature.

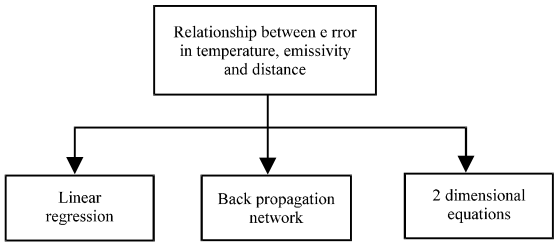

Fig. 5: Tree diagram for mathematical relationship

In this study, linear regression analysis, ANN based analysis and curve fitting techniques are used for determining two dimensional equations (tree diagram in Fig. 5). Regression analysis is one of the statistical tools for analyzing the data.

Relationship between the two input parameters (emissivity and distance) and error in temperature is obtained as follows, hence, actual temperature is obtained with the following Eq. 2-5:

$$\text{Error in temperature} = 66.93149 + (-26.7561 \times \text{emissivity}) + (-30.5525 \times \text{distance}) \quad (2)$$

$$\text{Error in temperature} = 102.638 + (-97.9578 \times \text{emissivity}) + (-25.0364 \times \text{distance}) \quad (3)$$

$$\text{Actual temperature} = 66.93149 + (-26.7561 \times \text{emissivity}) + \text{hotspot temperature} \quad (4)$$

$$\text{Actual temperature} = 102.638 + (-97.9578 \times \text{emissivity}) + \text{hotspot temperature} \quad (5)$$

RESULTS AND DISCUSSION

From the Eq. 2-5, it is found that distance and emissivity affect the hotspot temperature. Negative co-efficient indicate that decrease in temperature as the distance and emissivity increases. However, the co-efficient values vary as new sets of inputs are given. Hence, it is necessary to optimize the co-efficient and provide a much general heat equation in terms of emissivity and distance for developing the utility chart. Hence, two dimensional heat equations is derived using an appropriate equation, Table 2 shows the data that is used for obtaining the two dimensional heat equation where a(i, j) represent the error in temperature in °C at ith emissivity and jth distance.

Relationship between distance, emissivity and hotspot temperature is given in Fig. 6. Equation 6 provides the relationship between error in temperature, distance and emissivity:

$$\text{Error in temperature} = p00 + p10 \times \text{emissivity} + p20 \times \text{distance}^2 + p11 \times \text{distance} \times \text{emissivity} + p02 \times \text{distance}^2 \quad (6)$$

$$\text{Actual temperature} = p00 + p10 \times \text{emissivity} + p20 \times \text{distance}^2 + p11 \times \text{distance} \times \text{emissivity} + p02 \times \text{distance}^2 + \text{hotspot temperature} \quad (7)$$

Table 2: Impact of distance and emissivity on error in temperature

Emissivity/distance (m)	1	2	3
0.1	30.604	-4.838	-22.45
0.2	34.920	-5.750	-20.89
0.3	34.182	-5.535	-18.66
0.4	34.665	-2.946	-19.93
0.5	41.191	-7.889	-20.72
0.6	9.396	-14.590	-22.86
0.7	9.013	-14.590	-23.23
0.9	12.147	-11.930	-24.20
1.0	6.678	-15.150	-25.36

Where:
p00 = 99.29
p10 = -35.63
p01 = -70.96
p20 = -11.34
p11 = 15.15
p02 = 10.05

ANN based prediction of error in temperature: back propagation network is a feed forward network that consists of input layer, hidden layer and output layer (Albin *et al*., 2014). In this network, weights are updated using gradient descent rule. Number of neurons in input layer is dependent on the number of input parameters and similarly the number of neurons in the output layer is dependent on the number of output parameters. On the other hand, number of hidden layers and neurons in each layer determines the accuracy of training. As the number of hidden layers increases, accuracy also increases but at the cost of computational complexity. Hence, the number of hidden layers and the neurons in each layer are chosen in such a way that there is a compromise between accuracy and computational complexity. Also, the output is dependent on learning an momentum parameters.

In this research work, a five layered neural network is designed with three hidden layers. Number of neurons in each hidden layer is 20, 10 and 5, respectively. The learning and momentum parameters are 0.2 and 0.3, respectively. An exemplar table is created with emissivity and distance as input parameters and error in temperature as output parameter (Table 3).

Neural network is trained with 50% of data and the remaining 50% of data is used for testing. Table 4, shows the relationship between the desired and actual output for

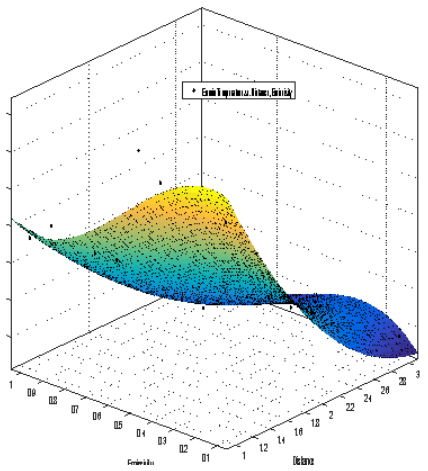

Fig. 6: Impact of distance and emissivity on error in temperature

Table 3: Exemplar generation

Input parameters		Output parameters
Emissivity	Distance (m)	Error in temperature (°C)
0.2	1	0.349200
0.4	1	0.346650
0.6	1	0.093960
0.8	1	0.087850
1.0	1	0.066780
0.2	2	-0.057500
0.4	2	-0.029460
0.6	2	-0.145900
0.9	2	-0.119300
0.1	3	-0.224500
0.3	3	-0.186600
0.5	3	-0.207200
0.7	3	-0.232300
0.9	3	-0.242000
0.1	1	0.845212
0.1	0.8	0.855805
0.2	0.7	0.647030
0.2	0.9	0.668899
0.4	1	0.282383
0.4	0.8	0.015167
0.8	1	-0.047520
0.8	0.8	6.80E-05
1.0	0.7	-0.040640
1.0	0.9	-0.043400

Table 4: Relationship between actual and desired output (Test dataset)

Input parameters		Error in temperature (°C)	
Emissivity	Distance (m)	Actual output	Desired output
0.2	1	0.349200	0.680758
0.4	1	0.346650	0.133476
0.6	1	0.093960	0.021052
0.8	1	0.087850	0.003203
1	1	0.066780	-0.043180
0.2	2	-0.057500	-0.043840
0.4	2	-0.029460	-0.042780
0.6	2	-0.145900	-0.078400
0.9	2	-0.119300	-0.712610
0.1	3	-0.224500	-0.187010
0.3	3	-0.186600	-0.272760
0.5	3	-0.207200	-0.242790
0.7	3	-0.232300	-0.413160
0.9	3	-0.242000	0.250175
0.1	1	0.845212	0.310556
0.1	0.8	0.855805	0.929562
0.2	0.7	0.647030	0.606982
0.2	0.9	0.668899	0.689447
0.4	1	0.282383	0.133476
0.4	0.8	0.015167	0.156543
0.8	1	-0.047520	0.003203
0.8	0.8	6.80E-05	0.012020
1	0.7	-0.040640	-0.029750
1	0.9	-0.043400	-0.070500

the test dataset. Relationship between the actual and the desired output for both trained and test dataset are shows in Fig. 7.

From the Fig. 7 it is found that actual and desired values are exactly the same for the trained dataset. However, for the test dataset there is a deviation between the actual and desired output. Mean square error between the desired and actual value is 0.0483.

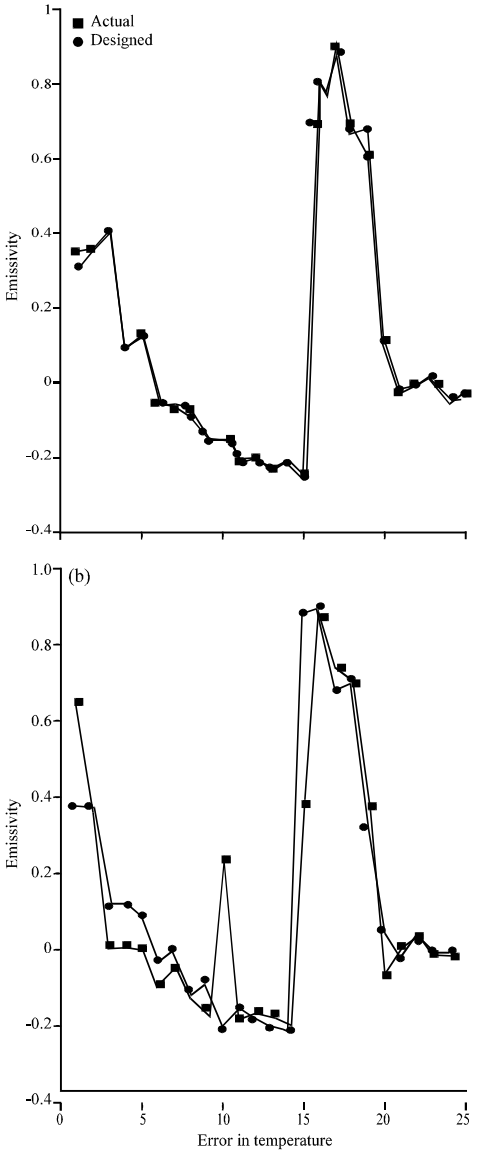

Fig. 7: Relationship between desired and actual output; a) Trained dataset and b) Test dataset

CONCLUSION

In this study, the utility chart for obtaining the actual temperature from thermographs has been successfully developed. Three different techniques namely linear regression, neural networks and curve fitting are discussed to obtain the two dimensional equation for actual temperature in terms of emissivity and distance. Though linear regression analysis provides a two dimensional equations, the constants are dependent on the number of datasets. Both neural network based technique is strongly dependant on the dataset used for training the network. Also, it is dependent on the number

of hidden layer neurons, learning parameter and momentum parameter. In this research, all the above parameters are optimizing heuristically. The research work can be extended by including the other IR camera parameters, namely, focal length, angle of acquisition, etc. Also, hardware can be developed for determining the actual temperature from thermographs.

REFERENCES

Albin, A.J., N.M. Nandhitha and S.E. Roslin, 2014. Text independent speaker recognition system using back propagation network with wavelet features. Proceedings of the 2014 International Conference on Communications and Signal Processing (ICCSP14'), April 3-5, 2014, IEEE, Melmaruvathur, India, ISBN:978-1-4799-3357-0, pp: 592-596.

Bedir, I., A.M. Azmy and F. Selim, 2013. High quality circuit breakers thermal inspections. Intl. J. Control Autom. Syst., 2: 19-33.

Bilodeau, G.A., R. Ghali, S. Desgent, P. Langlois and R. Farah *et al.*, 2011. Where is the rat? Tracking in low contrast thermographic images. Proceedings of the 2011 IEEE Computer Society Conference on Computer Vision and Pattern Recognition Workshops (CVPRW'11), June 20-25, 2011, IEEE, Colorado Springs, Colorado, ISBN:978-1-4577-0529-8, pp: 55-60.

Maldague, X.P., 2002. Introduction to NDT by active infrared thermography. Mater. Eval., 60: 1060-1073.

Sangeetha, M.S. and N.M. Nandhitha, 2016. Multilevel thresholding technique for contrast enhancement in thermal images to facilitate accurate image segmentation. Indian J. Sci. Technol., 9: 1-7.

Sangeetha, M.S. and N.M. Nandhitha, 2017. Improved active contour modelling for isolating different hues in infrared thermograms. Russ. J. Nondestr. Test., 53: 142-147.

Sangeetha, M.S., N.M. Nandhitha and S.E. Roslin, 2014. Impact of emissivity on the hotspot temperature for condition monitoring of electrical equipments in closed room. Adv. Mater. Res., 985: 1214-1219.

Schulz, R., S. Verstockt, J. Vermeiren, M. Loccufier and K. Stockman *et al.*, 2014. Thermal imaging for monitoring rolling element bearings. Proceedings of the 12th International Conference on Quantitative InfraRed Thermography (QIRT'14), July 7-11, 2014, University of Bordeaux, Bordeaux, France, pp: 1-9.

Suomela, J., 2012. Condition monitoring of paper machine with thermal imaging. Proceedings of the 24th SPIE Conference on Thermosense Vol. 4710, March 15, 2002, SPIE, Orlando, Florida, USA., pp: 143-151.

Ullah, I., F. Yang, R. Khan, L. Liu and H. Yang *et al.*, 2017. Predictive maintenance of power substation equipment by infrared thermography using a machine-learning approach. Energies, 10: 1987-1999.